Quantum dynamics of matter waves in a pulsed disordered lattice

Bryce Gadway,* Jeremy Reeves, Ludwig Krinner, and Dominik Schneble
Department of Physics and Astronomy, Stony Brook University, Stony Brook, NY 11794-3800, USA
(Dated: February 27, 2013)

We experimentally study the dynamical response of weakly-interacting atomic matter waves to a periodically pulsed, disordered optical lattice potential consisting of two overlapping standing-waves of incommensurate spatial periodicity. For periodic driving with a single standing wave only, we observe behavior consistent with the kicked-rotor model, namely ballistic spreading of momentum wavepackets at quantum resonances, and dynamical localization otherwise. However, adding the second standing wave can greatly modify these two effects. In particular, we find that the addition of disorder destroys dynamical localization when the driving is off-resonant and suppresses delocalization for a resonant drive. Our findings directly relate to quantum localization phenomena in low-dimensional systems, and illustrate the role of decoherence in the dynamics of driven quantum systems.

PACS numbers: 05.45.-a ; 05.45.Mt ; 67.85.Hj ; 61.43.-j

In isolated ultracold atomic systems, the quantum nature of matter can be made manifest in sometimes striking and counterintuitive ways. One example of distinctly quantum behavior arises in the dynamics of quantum systems whose classical counterparts are chaotic, i.e. so-called *quantum chaotic* systems, where destructive interference can suppress the onset of chaos [1]. The δ-kicked rotor model [1] has found particular relevance in experimental studies of driven quantum particles, as realized with cold neutral atoms periodically kicked by trains of optical standing wave pulses [2]. Whereas regimes of fully chaotic behavior with diffusive growth of the momentum variable can be found in the classical system, the quantum analog generically displays dynamical localization in momentum space due to quantum interference [1, 3, 4], which has been shown [5] to be analogous to one-dimensional (1D) Anderson localization [6] in configuration space. Studies of the contrasting dynamics of classical and quantum systems, and in particular those addressing how classical behavior can arise in the presence of noise [7–11] and nonlinearities [12–15], are central to the understanding and control of quantum decoherence [16].

Foundational experimental studies of quantum chaos in driven cold atomic vapors [2, 17] have demonstrated dynamical localization. Moreover, recent progress has even allowed for the investigation of analogs to 3D Anderson localization in these systems [18, 19], as well as of the influence of noise and decoherence on quantum dynamics [20–22]. Other recent studies of δ-kicked rotor dynamics with atomic matter-waves have allowed for clear observations of resonant dynamics [23, 24] when the pulse period corresponds to a discrete energy resonance in the system. Such resonantly pulsed matter-wave systems should also allow for studies of quantum decoherence, owing to their connection to quantum random walks [25].

In this manuscript, we explore the effects of controlled disorder on the dynamics of a quantum kicked rotor system, as realized with ultracold atomic matter waves in a periodically pulsed optical lattice. We observe that effects linked to interference in the quantum kicked rotor model, namely linear momentum growth at quantum resonances and dynamical localization for off-resonant driving, are largely destroyed due to the addition of disorder. These observations suggest a breakdown in the quantum dynamics of driven particles under the influence of noise, corresponding to a quantum-to-classical transition in open systems. Moreover, our observation of

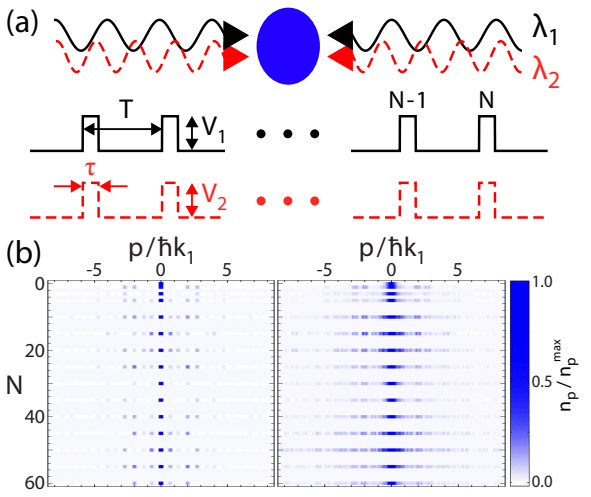

FIG. 1. Atomic matter waves in a periodically-pulsed standing wave field. (a) A cloud of ultracold atoms is exposed to two incommensurate optical standing waves with wavelengths $\lambda_{1,2}$ and spatial frequencies $k_{1(2)} = 2\pi/\lambda_{1(2)}$, whose intensities are repeatedly pulsed on for a short time τ at a periodic spacing T. (b) Time-of-flight momentum spectra, theoretical (left) and experimental (right), of matter waves after N kicks from off-resonantly pulsed optical standing waves of absolute depths $V_1 = V_2 = 50E_R$, with E_R the energy of atoms recoiling with momentum $\hbar k_1$.

disorder-induced transport for off-resonant driving has connections to Anderson localization in low-dimensional systems, as well as to transport in quasicrystalline materials [26].

Our system consists of a nearly-pure Bose–Einstein condensate (BEC) of $(1.4 \pm 0.4) \times 10^5$ ^{87}Rb atoms in the $|F, m_F\rangle = |2, -2\rangle$ hyperfine ground state. The atoms are fully supported against gravity by a compensating magnetic field gradient, and are loosely trapped in a crossed-beam optical dipole trap of wavelength 1064 nm. The trapping potential has a mean harmonic frequency $\omega_{HO}/2\pi \approx 20$ Hz, and the BEC has a chemical potential $\mu/h \approx 0.3$ kHz. To realize the quantum kicked rotor model, the atoms are driven by pulsed optical lattices oriented along the z-axis, as depicted in Fig. 1 (a). We perform simultaneous pulsing by two optical lattices of wavelengths $\lambda_1 = 1064$ nm and $\lambda_2 = 782$ nm, and corresponding wavevectors $k_{1(2)} = 2\pi/\lambda_{1(2)}$. The lattice depths are characterized as $V_{1(2)} = s_{1(2)}E_R$ (with $E_R = \hbar^2 k_1^2/2M$ the recoil energy of the first lattice and M the atomic mass), and are calibrated by Kapitza–Dirac diffraction [27]. Subsequently, we use short pulses of length $\tau = 2$ μs (Raman–Nath regime), spaced at a pulse period T that is varied to investigate either resonant or off-resonant dynamics. After applying a train of N lattice pulses to the BEC, we immediately release the atoms and allow them to freely evolve in time-of-flight (TOF) for 16 ms before performing absorptive imaging of momentum distributions, as displayed in Fig. 1 (b).

The system subject to a train of N lattice pulses is approximately [28] described by the 1D Hamiltonian $H = -(\hbar^2/2M)\partial^2/\partial z^2 + S(t)E_R$, with $S(t) = [s_1 \cos^2(k_1 z) + s_2 \cos^2(k_2 z)] \sum_{j=1}^{N} \Pi(t/\tau - jT/\tau)$, where Π is a unit-step function. By approximating the pulses as δ-functions, the Hamiltonian can be recast as that of a δ-kicked rotor [2], $H' = \rho^2/2 + K(\phi) \sum_{j=1}^{N} \delta(t' - j)$, with $K(\phi) = K_1 \cos(\phi) + K_2 \cos(\eta\phi)$ and η defined by the ratio $k_2/k_1 \sim 1.36$, and rescaled quantities $t' = t/T$, $H' = (4k_1^2 T^2/M)H$, $\phi = 2k_1 z$, $\rho = (2k_1 T/M)p$. Here, the conjugate variables ϕ and ρ obey the commutation relation $[\phi, \rho] = i\kappa$, with an effective Planck constant $\kappa = 8E_R T/\hbar = 8T/T_R$ (recoil time $T_R = \hbar/E_R$). The so-called *stochasticity* parameters $K_{1(2)} = 4s_{1(2)}\tau T/T_R^2$ serve to delineate regimes of classically regular and chaotic motion. Resonant driving by the first (second) lattice is achieved when $\kappa/4\pi$ ($\eta^2\kappa/4\pi$) is equal to a rational number [or in the parlance of Talbot interference [24], when T matches a rational multiple of the Talbot time $T_T = T_R\pi/2$ ($T_R\pi/2\eta^2$)].

We begin our studies by investigating the effects of disorder on dynamical localization in momentum space [2], using a pulse period of $T = 36$ μs that corresponds to off-resonant driving for each of the two lattices. For kicking with only a single lattice [$K_{1(2)} = 2.3(0)$], we find that the population remains trapped in momentum space with increasing kick number N, such that in Fig. 2 (a) we observe apart from fluctuations no sustained growth in the per-particle energy ε (in units of E_R). However, we see in Fig. 2 (b) that when we switch to a strong incommensurate lattice potential ($K_1 = K_2 = 2.3$) the dynamical localization is destroyed and the population spreads out in momentum space, leading to an increase in kinetic energy. Such a deviation from the dynamics of the standard kicked rotor, namely a transition from dynamical localization to delocalization, has been predicted for cold atoms periodically pulsed with incommensurate standing waves [10], and it was proposed that for irrational values of η this growth can be unbounded.

To compare our experimental results to theory, we directly simulate the matter-wave dynamics due to evolution under H, considering a basis of plane-wave momentum states coupled by the two light fields of the form $|m, n\rangle$, having momentum $p_{m,n}/\hbar k_1 = 2m + 2n\eta$. We start with all population in the zeroth momentum order, i.e. $|\psi_0\rangle = |0, 0\rangle$, and then describe the total evolution from one pulse to the next by a unitary "kick" opera-

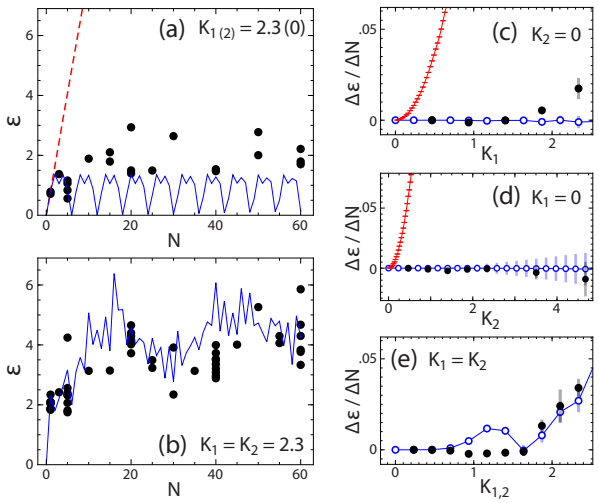

FIG. 2. Dynamical evolution of matter waves under off-resonant kicking in the presence of disorder. (a) The atoms' per-particle energy ε as a function of the number of kicks N. The atoms are kicked by only a single lattice potential, with stochasticity parameter $K_1 = 2.3$, resulting in dynamical localization or a lack of growth in ε. Black points are experimental data, the blue solid line and red dashed lines are simulated quantum and classical trajectories, as detailed in the text. (b) When an incommensurate, disordering lattice is added ($K_2 = 2.3$), the dynamical localization is destroyed, and growth in the energy ε is observed. (c,d,e) The rate of energy growth with kick number, $\Delta\varepsilon/\Delta N$, as determined from linear fits to experimental data and theory points. Filled black points are experimental, open blue disks are theory, and error bars represent the standard error of the linear fits. Shown are the cases of (c) only the first lattice with $K_2 = 0$, (d) only the second lattice with $K_1 = 0$, and (e) both lattices present with the same strength of kicking $K_1 = K_2$. Red points in (c,d) are classical growth rates.

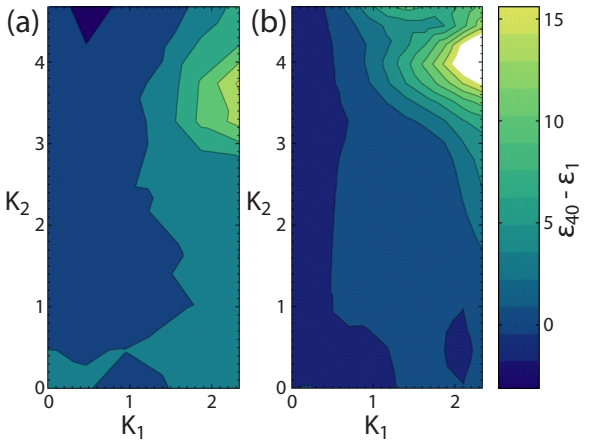

FIG. 3. Energy growth under simultaneous off-resonant driving from two optical fields. (a) Experimentally measured change in energy ε from $N = 1$ to 40 kicks as a function of the stochasticity parameters K_1 and K_2, for a pulse period $T = 36$ μs that is off-resonant for each lattice. (b) Change in mean per-particle energy from numerical simulations.

tor $\hat{U}$ [29]. After a train of N pulses, the final atomic wavefunction is given by $|\psi_N\rangle = \hat{U}^N|\psi_0\rangle$. From the simulated momentum distributions, we calculate both the mean per-particle energy ε (in units of E_R) and the rms momentum width σ_p (in units of $\hbar k_1$) [30]. As shown in Fig. 2 (a,b), we find in general good agreement between the experimental measurements and the theoretical quantum trajectories, which rely on no free parameters. To demonstrate that the relative lack of growth in the single lattice case is due to dynamical localization and not to classical localization (KAM barriers separating classically chaotic regions [31]), we also show in Fig. 2 (a) the classical energy growth as averaged over 10^5 trajectories [32], which is nearly linear with N.

Given the experimental restriction to relatively low values of N, and the appearance of non-trivial oscillatory behavior as in Fig. 2 (b), we abstain from attempting to discern fine details of the energy growth (e.g. subdiffusive vs. diffusive). However, to gain some insight into the apparent disorder-driven crossover from localization to delocalization, we characterize the energy-growth per kick $\Delta\varepsilon/\Delta N$ using a simple linear fit to the energy evolution (for $1 \leq N \leq 60$, allowing for an energy offset after the first kick). The rates of growth as a function of the stochasticity parameters are plotted in Fig. 2 (c–e) for the cases $K_1 = 0$, $K_2 = 0$, and $K_1 = K_2$. We see in Fig. 2 (c,d) no sustained growth for either of the single-lattice cases. We again rule out classical localization effects by comparing to the linear growth rates of classical energy trajectories as plotted in Fig. 2 (c,d). When we kick simultaneously with both lattices, however, we observe a transition to a regime of growth in Fig. 2 (e), both in experiment and in the simulations (with a region of weak transient growth near the transition, seen in the theoretical curves but not in experiment).

To obtain a more complete picture of the dependence of dynamical localization on the two lattice strengths, we now more fully sample the available parameter-space of K_1 and K_2. In Fig. 3 (a,b) we show both experimental and theoretical results for the change in the kinetic energy ε between $N = 1$ and 40 kicks, with good qualitative agreement. As expected, growth is minimal along either of the two axes, where only a single lattice is predominantly used, while significant growth is achieved when strongly driving the atoms with the two incommensurate lattices. A deeper understanding of the mechanism associated with this growth may be found by considering analogies to atoms driven along one dimension by standing waves at multiple *temporal* frequencies [9, 18, 19, 33]. In our scenario with multiple *spatial* frequencies, the kicking with only one lattice as in Fig. 2 (c,d) would hence relate to Anderson localization in 1D, while 2D localization is achieved by kicking equally with both lattices as in Fig. 2 (e). Fig. 3 (a,b) thus displays the crossover between these two limits. Signatures of such a crossover in the $K_1 - K_2$ plane between dynamical localization and delocalization can also be obtained through an analysis of the kick operator $\hat{U}$ that is independent of the kick number [32], based on a stroboscopic Floquet state analysis [5, 34]. Along the line $K_1 = K_2$, such an analysis reveals a transition to delocalized states at a value $K_{1,2} \sim 2.2$, in approximate agreement with our observations in Fig. 2 (e). Lastly, we note the formal similarity between our observation of delocalization in momentum-space induced by pulsed disorder and the recent observation of disorder-enhanced transport in photonic quasicrystals [26], in which the increased density of states plays an important role in promoting transport. Similarly, when the atoms' momentum modes are coupled by both of the incommensurate optical lattices, the energy spacing between adjacent occupiable modes is greatly reduced.

We now turn to investigate the effect of disorder on the dynamics of a resonantly-kicked quantum rotor. For this purpose, the use of ultracold atoms with large de Broglie coherence length is vital, so as to avoid trivial decoherence due to spatial separation of the momentum components. To achieve a resonance condition for the first lattice, we set the pulse period to $T = 124$ μs, such that $\kappa/4\pi \sim 1$. Even for a weak optical potential ($K_1 = 1.6$; $s_1 = 10$), we observe in Fig. 4 (a) a linear increase in the momentum width of an ensemble of resonantly kicked atoms for up to $N = 20$. We note roughly a factor of 2 difference in the growth rate from what we expect based on plane-wave simulations. This deviation can be explained through the finite size of the trapped atomic distribution (Thomas–Fermi radius ~ 9 μm along z), which gives rise to an initial rms momentum spread $\Delta p/\hbar k_1 \approx 0.03$. We plot in Fig. 4 (a) the expected on-resonance momentum growth, as averaged over the initial

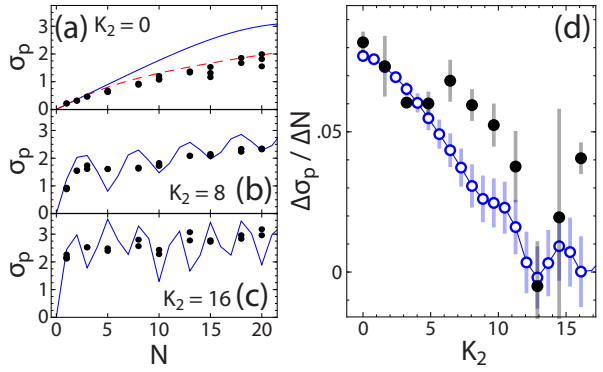

FIG. 4. Dynamical evolution of resonantly driven matter waves in the presence of disorder. (a) The momentum-width σ_p of the atomic distribution as a function of kick number N, for resonant driving of the first lattice at a pulse period of $T = 124$ μs. When kicked by only a single resonant standing wave ($K_1 = 1.6$), a near linear increase in σ_p is observed. Black points are data from individual experimental realizations, the solid blue line is a numerical calculation for an initial plane-wave state, while the dashed red analytical curve takes into account the initial momentum-width of the atomic distribution due to finite-size. (b,c) Similar traces of the momentum-width as a function of N with added disorder, due to a strong incommensurate lattice potentials ($K_2 = 8, 16$). (d) The growth rate of the momentum-width, $\Delta\sigma_p/\Delta N$, as determined by a linear fit to the dependence on N, is observed to decrease with increasing strength of the incommensurate lattice K_2. The growth rates determined from theory (open blue circles) are scaled by a factor of 1/2 to account for effects of the initial spread in momentum.

momentum distribution of the sample [35]. To investigate the effects of disorder, we now add deep off-resonant, incommensurate lattices of strength $K_2 = 8$ and 16 as shown in Fig. 4 (b,c). While adding them leads to very large initial momentum widths after the first kick, the rates of momentum growth thereafter are found to be markedly less than in the single-lattice case. We again characterize the growth rate $\Delta\sigma_p/\Delta N$ by a simple linear fit in the range $1 \leq N \leq 20$, and these values are plotted in Fig. 4 (d) as a function of the second, disordering lattice strength K_2. We observe a trend towards inhibited growth with an increasing amount of disorder, in agreement with the theoretical prediction. Such a breakdown of coherent growth in the momentum width due to added disorder is consistent with the observed destruction of dynamical localization, which also relied on quantum interferences. The observed sensitivity of resonant dynamics to spatial frequency noise mirrors the effects of decoherence by spontaneous emission on quantum resonances [21].

In conclusion, we have studied quantum kicked rotor dynamics in the presence of controlled disorder, using an ensemble of ultracold atoms driven by two incommensurate optical lattices. In the absence of disorder, we observe both a coherent growth in momentum when the pulse period corresponds to a quantum resonance, as well as dynamical localization in momentum space when the pulsing is off-resonant. We observe that the addition of disorder destroys dynamical localization and leads to momentum growth for off-resonant driving, while also suppressing the growth in momentum space for resonantly-kicked rotors. Our observations highlight the fragile nature of effects relying on quantum interference, as well as the transition from quantum to classical behavior due to environmental coupling.

Possible extensions of our study include the realization of kicked harmonic oscillators [36, 37] with strong nonlinear couplings, e. g. by studying the single-site orbital dynamics of a periodically-tilted Mott insulator with tunable filling and interaction strength, or the study of the anomalous quantum Hall effect with a spinful version of the quantum kicked rotor [38], as may be realized with cold atom mixtures in a spin-dependent lattice [39].

We thank Martin G. Cohen and Thomas Bergeman for valuable comments on the manuscript, and Mikael Rechtsman for discussions. This work was supported by NSF (PHY-0855643) and the Research Foundation of SUNY. B.G. and J.R. acknowledge support from the GAANN program of the US DoEd.

* bgadway@ic.sunysb.edu

[1] G. Casati *et al.*, "Stochastic behavior in classical and quantum hamiltonian systems," (Springer, New York, 1979) p. 334
[2] F. L. Moore *et al.*, Phys. Rev. Lett. **75**, 4598 (1995)
[3] T. Hogg and B. A. Huberman, Phys. Rev. Lett. **48**, 711 (1982)
[4] S. Fishman, D. R. Grempel, and R. E. Prange, Phys. Rev. Lett. **49**, 509 (1982)
[5] D. R. Grempel, R. E. Prange, and S. Fishman, Phys. Rev. A **29**, 1639 (1984)
[6] P. W. Anderson, Phys. Rev. **109**, 1492 (1958)
[7] D. L. Shepelyansky, Physica **8D**, 208 (1983)
[8] E. Ott, T. M. Antonsen, and J. D. Hanson, Phys. Rev. Lett. **53**, 2187 (1984)
[9] G. Casati, I. Guarneri, and D. L. Shepelyansky, Phys. Rev. Lett. **62**, 345 (1989)
[10] R. Graham and A. R. Kolovsky, Physics Letters A **222**, 47 (1996)
[11] S. Adachi, M. Toda, and K. Ikeda, Phys. Rev. Lett. **61**, 659 (Aug 1988)
[12] F. Benvenuto *et al.*, Phys. Rev. A **44**, R3423 (1991)
[13] D. L. Shepelyansky, Phys. Rev. Lett. **70**, 1787 (1993)
[14] C. Zhang *et al.*, Phys. Rev. Lett. **92**, 054101 (2004)
[15] G. J. Duffy *et al.*, Phys. Rev. A **70**, 041602 (2004)
[16] W. H. Zurek, Physics Today **44**, 36 (1991)
[17] E. J. Galvez *et al.*, Phys. Rev. Lett. **61**, 2011 (1988)
[18] J. Chabé *et al.*, Phys. Rev. Lett. **101**, 255702 (2008)
[19] G. Lemarié *et al.*, Phys. Rev. Lett. **105**, 090601 (2010)
[20] B. G. Klappauf *et al.*, Phys. Rev. Lett. **81**, 1203 (1998)
[21] M. B. d'Arcy *et al.*, Phys. Rev. Lett. **87**, 074102 (2001)
[22] M. B. d'Arcy *et al.*, Phys. Rev. E **64**, 056233 (2001)

[23] L. Deng *et al.*, Phys. Rev. Lett. **83**, 5407 (1999)
[24] C. Ryu *et al.*, Phys. Rev. Lett. **96**, 160403 (2006)
[25] A. Romanelli *et al.*, Physica A **352**, 409 (2005)A. Romanelli, R. Siri, and V. Micenmacher, Phys. Rev. E **76**, 037202 (2007)
[26] L. Levi *et al.*, Science **332**, 1541 (2011)
[27] B. Gadway *et al.*, Opt. Express **17**, 19173 (2009)
[28] We ignore effects of nonlinear interactions and the weak trapping potential, as the total pulse duration is kept less than both h/μ and $2\pi/\omega_z$, where $\omega_z \approx 2\pi \times 30$ Hz is the trap frequency along the direction of kicking. The pulses are approximated as step functions, while the actual intensity profiles are smoother but with an equivalent area
[29] $\hat{U} = \hat{R}^{-1}\hat{E}_L\hat{R}\hat{E}_0$, where $\hat{E}_0$ accounts for free evolution for a time $T - \tau$. $\hat{E}_L$ describes evolution of the lattice eigenstates (as determined by numerical diagonalization) during the pulse for a time τ. $\hat{R}$ maps the free-particle eigenstates onto those of the lattice
[30] While we consider up to ± 15 momentum orders for each laser field, we restrict the determination of ε and σ_p to the region $|p|/\hbar k_1 \leq 15$, to be in agreement with the range of experimentally observed momenta
[31] T. Geisel, G. Radons, and J. Rubner, Phys. Rev. Lett. **57**, 2883 (1986)
[32] See Supplementary Material for more information on determination of classical dynamics, as well as a time-independent analysis of the kick operator $\hat{U}$
[33] J. Ringot *et al.*, Phys. Rev. Lett. **85**, 2741 (2000)
[34] G. Lemarié *et al.*, Phys. Rev. A **80**, 043626 (2009)
[35] For simplicity we assume a Gaussian distribution with momentum width $0.03\hbar k_1$, and use Eq. (2) from Ref. [24] (Eq. (13) of Ref. [40]) describing the dependence of the energy growth rate on initial momentum
[36] R. Lima and D. Shepelyansky, Phys. Rev. Lett. **67**, 1377 (1991)
[37] I. Dana, Phys. Rev. Lett. **73**, 1609 (1994)
[38] J. P. Dahlhaus *et al.*, Phys. Rev. B **84**, 115133 (2011)
[39] D. Pertot, B. Gadway, and D. Schneble, Phys. Rev. Lett. **104**, 200402 (2010)
[40] S. Wimberger *et al.*, Nonlinearity **16**, 1381 (2003)

Supplementary Material to "Quantum dynamics of matter waves in a pulsed disordered lattice"

Bryce Gadway, Jeremy Reeves, Ludwig Krinner, and Dominik Schneble

Department of Physics and Astronomy, Stony Brook University, Stony Brook, NY 11794-3800, USA

CLASSICAL DYNAMICS

It is well known that classical localization can occur in kicked-rotor systems for small values of the stochasticity parameter, where the classical system is not globally chaotic but supports bounded orbits due to Kolmogorov-Arnol'd-Moser (KAM) barriers [1]. To demonstrate that this effect does not contribute to the observed localization in momentum space in Fig. 2 (a,c,d) of the main text (i.e. for atoms kicked by only a single optical lattice), we compare the experimental data and the simulated quantum trajectories of the per-particle energy ε as a function of kick number N to simulated classical dynamics, averaged over 10^5 classical trajectories. To briefly detail the determination of the averaged classical dynamics, each individual classical trajectory is determined by probabilistically projecting out the particle's momentum-space wavefunction after each application of the kick operator $\hat{U}$. We show in FIG. A (i-iv) the classical dynamics of ε, as averaged over $n = 10$, 10^2, 10^3, and 10^5 individual trajectories, for the same system parameters as used in Fig. 2 (a) of the main text [$T = 36$ μs ; $\tau = 2$ μs ; $K_1 = 2.3$ ($s_1 = 50$) ; $K_2 = 0$]. For large sample sizes, the classical growth rate is found to be in good agreement with the expected classical diffusion constant [2], $\Delta\varepsilon/\Delta N \sim V_1^2\tau^2/2\hbar^2 = 2K_1^2/\kappa^2$, for the first lattice ($2\eta^2K_2^2/\kappa^2$ for the second lattice). We have verified that the slight deviation between the growth rate of simulated classical trajectories and the expected classical diffusion is due to the finite length ($\tau = 2$ μs) of the lattice pulses.

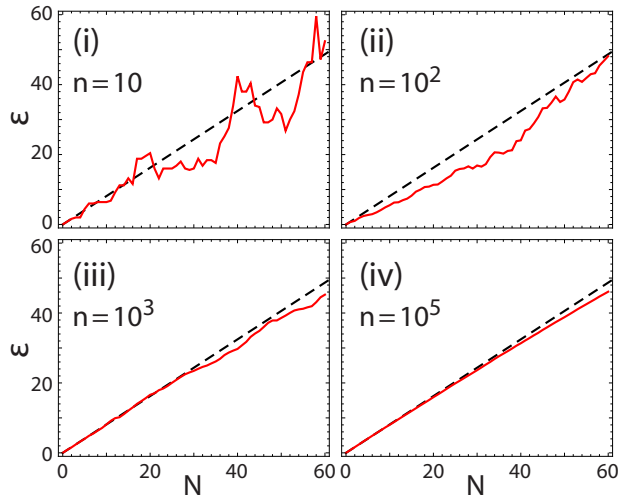

FIG. A. Averaged classical dynamics of the energy ε as a function of kick number N for different sample sizes consisting of n trajectories, for off-resonant kicking with the first lattice [$K_1 = 2.3$ ($s_1 = 50$) ; $K_2 = 0$]. (i-iv) Averaged trajectories are shown for the cases of $n = 10$, 10^2, 10^3, and 10^5 as solid red lines. In all plots, we also show as a dashed black line the expected classical diffusion for delta-function kicks.

FLOQUET EIGENSTATE ANALYSIS OF $\hat{U}$

To gain a deeper insight into the expected response of the matter waves to a given kick operator $\hat{U}$ (i.e. for given pulse lengths, lattice depths, and pulse period), we analyze the properties of the matrix $\hat{U}$ in a time-independent manner. While monitoring the response of the matter waves as a function of the kick number N makes a direct connection to experiment and can discern between regimes of localization and delocalization in momentum-space through the long-term growth dynamics, at short times it may be subject to transient behavior and small-scale fluctuations. We are experimentally restricted to a modest number of kicks to maintain a near-field treatment (assuming identical, overlapped spatial wavefunctions for all the matter-wave fields) and to minimize contributions from nonlinear atom-atom interactions. Motivated by pioneering work that made a stroboscopic connection between the quantum δ-kicked rotor model and the 1D Anderson model on a lattice [1], we study the properties of the Floquet (or Bloch–Floquet) quasi-energy eigenstates of the kick operator $\hat{U}$. For regimes in which the growth dynamics result in dynamical localization, these Floquet eigenstates should all be localized in momentum space, while they are delocalized in the case of diffusive growth.

We first investigate the case of kicking off-resonantly with two lattices of equal strength, using the same parameter values as in Fig. 2 (e) of the main text, with variable stochasticity parameter $K_1 = K_2 \equiv K_{1,2}$. In Fig. B (i,ii), we plot the momentum-space distribution of the lowest energy Floquet eigenstates of $\hat{U}$, $|\psi_0^U\rangle$, for the values $K_{1,2} = 2.15$ and 2.34. The plotted distributions are shifted by the mean momentum $\bar{p} = \langle\psi_0^U|\hat{p}|\psi_0^U\rangle$ to $p' = p - \bar{p}$. While the distribution is localized for the weaker kicking strength, it is delocalized into two regions for the larger strength. In fact, in Fig. B (iii) we observe a bifurcation of the eigenstate distributions as the stochasticity parameter $K_{1,2}$ is increased. We can readily calculate the rms momentum width $\sigma_{p'}$ of these distributions, and as shown in Fig. B (iv) there is a sharp rise in the width across a value of $K_{1,2} \sim 2.2$. Not surprisingly, this value is in general agreement with the observed onset of non-zero energy growth versus kick number in Fig. 2 (e) of the main text.

Further motivated by the connection of our experiment involving atoms driven with two *spatial* frequencies to experiments performed with multiple *temporal* frequencies, which result

in an effectively higher-dimensional localization when the frequencies are incommensurate, we can also perform a Floquet eigenstate analysis in the full parameter space of K_1 and K_2. In Fig. C (i), we plot as white the regions in which the Floquet eigenstates are localized in momentum space and as dark blue the regions in which they are delocalized, with the criterion for delocalization being that more than 10% of the population resides further than 5.5 momentum units ($\hbar k_1$) away from the most populated mode. This plot shows localization along either axis, where dynamical localization is expected for any value of the kicking strength when only a single lattice is used, while delocalization generally occurs beyond some line in the parameter space spanned by K_1 and K_2. If the expected connection to the scenario of driving with multiple temporal frequencies holds, this would be analogous to the phase diagram of the anisotropic 2D Anderson model, in which the pseudo-randomness of the site energies is provided by the fact that the pulse period does not match the Talbot time of either lattice, such that the relative kick strengths K_1 and K_2 give rise to off-diagonal terms that cause "tunneling" between momentum states. We also show in Fig. C (ii) the simulated change in ε between one and $N = 40$ kicks, as in Fig. 3 (b) of the main text but over a larger range of K_1 values. This plot demonstrates that qualitatively similar regions of localization and delocalization are also observed in the energy growth dynamics.

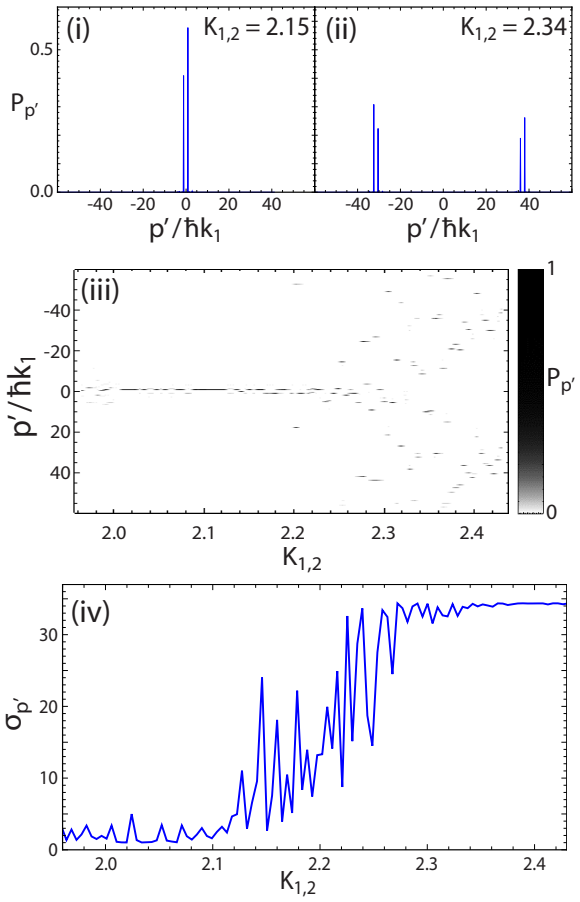

FIG. B. Time-independent analysis of the kick operator $\hat{U}$ for off-resonant kicking ($T = 36$ μs) by both lattices, with equal kicking strengths $K_{1,2}$ for each. (i,ii) The momentum distribution of the lowest energy Floquet eigenstate of $\hat{U}$, $|\psi_0^U\rangle$, in the plane-wave basis. The momenta p are shifted by the mean value $\bar{p} = \langle\psi_0^U|\hat{p}|\psi_0^U\rangle$ to $p' = p - \bar{p}$. For low values of the kicking strength, as in (i), the eigenstates are localized in momentum-space, while for larger values they became delocalized as in (ii). (iii) Momentum distributions as in (i,ii) as a function of the stochasticity parameter $K_{1,2}$. Beyond a value of $K_{1,2} \sim 2.2$ a bifurcation and delocalization of the momentum distributions is observed. (iv) For the same range of stochasticity parameter values as in (iii), we plot the rms momentum width $\sigma_{p'}$ of the lowest energy eigenstates of $\hat{U}$, which exhibits a sharp increase across a value $K_{1,2} \sim 2.2$.

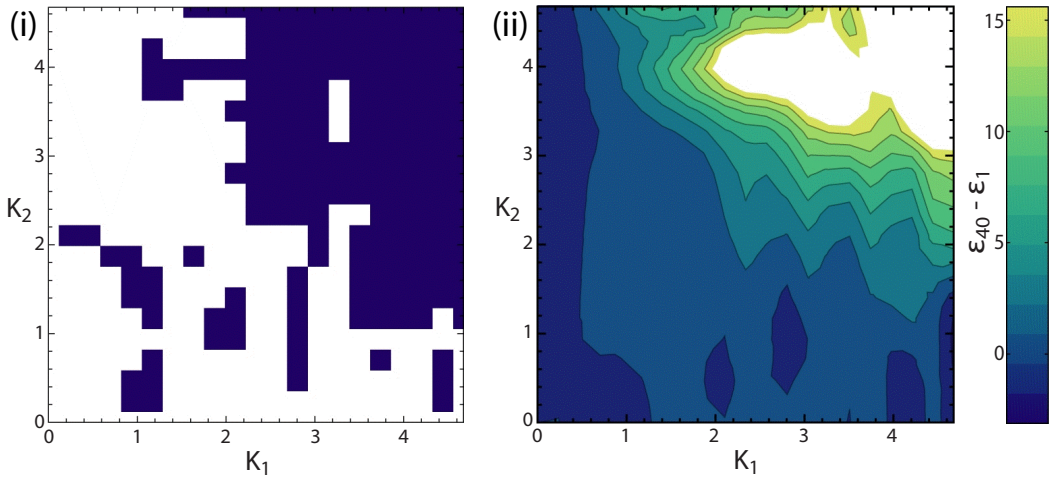

FIG. C. Localization-delocalization transition in the K_1-K_2 plane. (i) As a function of the stochasticity parameters K_1 and K_2, we plot as white the regions in which the Floquet eigenstates of $\hat{U}$ are localized in momentum-space and as blue the regions in which they are delocalized, as detailed in the text. A general trend of delocalization for strong kicking with both lattices, and localization when kicking with only a single lattice, is observed. (ii) Here we replot the simulation data from Fig. 3 (b) of the main text, showing the change in energy ε from the first to $N = 40$ kicks, but over a larger range of K_1 values. Behavior qualitatively similar to the localization-delocalization plot in (i) can be observed in this dynamical response data.

[1] D. R. Grempel, R. E. Prange, and S. Fishman, Phys. Rev. A **29**, 1639 (1984).

[2] G. Lemarié et al., Phys. Rev. A **80**, 043626 (2009).